

Formation and Stability of Mononuclear and Dinuclear Eu(III) Complexes and Their Catalytic Reactivity Toward Cleavage of an RNA Analog

Erik R. Farquhar, John P. Richard,* and Janet R. Morrow*

Department of Chemistry, University at Buffalo, State University of New York, Amherst, New York 14260-3000

Received March 24, 2007

The complex between Eu(III) and 1,7-diaza-4,10,13-trioxacyclopentadecane-*N,N*-diacetic acid (L4) was characterized by pH potentiometric titration and ^1H NMR spectroscopy. The conversion of the monomer to a dimeric complex is observed as the pH is increased from 7 to 10 in a reaction that releases one mol/ HO^- per dimer formed. The dimeric complex undergoes a further ionization with a $\text{p}K_{\text{a}}$ of 10.7. Kinetic parameters are reported for the cleavage of the simple phosphodiester 2-hydroxypropyl-4-nitrophenyl phosphate catalyzed by both the monomeric and the dimeric Eu(III) complexes. These data show that the monomer and dimer stabilize their bound reaction transition states with similar free energies of 7.1 and 7.6 kcal/mol, respectively. Clearly, a bridging hydroxide is not an optimal linker to promote cooperative catalysis between Eu(III) centers in macrocycles with multiple polyaminocarboxylate pendent groups.

Introduction

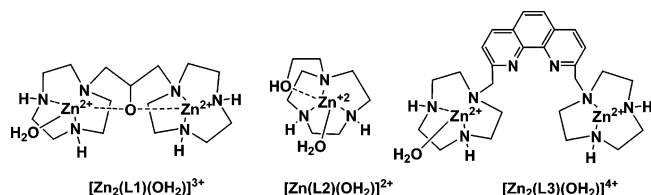
The development of rational approaches to the design of catalysts that stabilize the transition state for the cleavage of RNA to form a cyclic phosphate ester has proven to be problematic. There is an increase in charge from -1 to -2 at the reacting phosphate ester moiety of both RNA and analogs of RNA on proceeding from the reactant state to the transition state for the cleavage reaction. The electrostatic interaction between a metal cation and a bound substrate will provide relatively weak stabilization of the Michaelis complex of the substrate *monoanion* and greater stabilization of the *dianionic* transition state for phosphate diester cleavage.^{1–3} This prompts the simple-minded, but rational, proposal that the most effective catalysts of RNA cleavage will be those that interact most strongly with the transition-state dianion. In developing this proposal, we have previously shown that $[\text{Zn}_2(\text{L}1)(\text{OH}_2)]^{3+}$, with two Zn^{2+} ions drawn together by interaction with a bridging alkoxide anion, is a much better catalyst for the cleavage of several phosphate diesters, including a dinucleotide, than the corresponding mono-

nuclear catalyst, $[\text{Zn}(\text{L}2)(\text{OH}_2)]^{2+}$.^{4–6} The advantage of using a bridging alkoxide to link two Zn(II) ions has been demonstrated by other groups as well. For example, dinuclear Zn(II) complexes with pyridine donor groups and a bridging alkoxide are highly effective catalysts for cleavage of RNA analogs.^{7–9} By comparison, complexes that lack a bridging group do not have the two Zn(II) centers oriented to cooperatively catalyze cleavage. The catalytic activities of many simple tethered dinuclear Zn^{2+} complexes (e.g. $[\text{Zn}_2(\text{L}3)(\text{OH}_2)]^{4+}$) are only (2–5)-fold higher than the analogous mononuclear catalyst, $[\text{Zn}_2(\text{L}2)(\text{OH}_2)]^{2+}$.¹⁰ In contrast to these studies of catalysts in aqueous solutions, studies of dinuclear Zn(II) catalysts in solvents that are less polar and more weakly coordinating than water show effective catalysis in the absence of a linker with a bridging group, most likely

* To whom correspondence should be addressed. E-mail: jrmorrow@buffalo.edu (J.R.M.), jrjrichard@buffalo.edu (J.P.R.).

- (1) Yang, M.-Y.; Iranzo, O.; Richard, J. P.; Morrow, J. R. *J. Am. Chem. Soc.* **2005**, *127*, 1064–1065.
- (2) Feng, G.; Mareque-Rivas, J. C.; Martín de Rosales, R. T.; Williams, N. H. *J. Am. Chem. Soc.* **2005**, *127*, 13470–13471.
- (3) Feng, G.; Natale, D.; Prabakaran, R.; Mareque-Rivas, J. C.; Williams, N. H. *Angew. Chem., Int. Ed.* **2006**, 7056–7059.

- (4) O'Donoghue, A.-M.; Pyun, S. Y.; Yang, M.-Y.; Morrow, J. R.; Richard, J. P. *J. Am. Chem. Soc.* **2006**, *8*, 1615–1621.
- (5) Iranzo, O.; Kovalevsky, A. Y.; Morrow, J. R.; Richard, J. P. *J. Am. Chem. Soc.* **2003**, *125*, 1988–1993.
- (6) Iranzo, O.; Richard, J. P.; Morrow, J. R. *Inorg. Chem.* **2004**, *43*, 1743–1750.
- (7) Feng, G.; Natale, D.; Prabakaran, R.; Mareque-Rivas, J. C.; Williams, N. H. *Angew. Chem., Int. Ed.* **2006**, 7056–7059.
- (8) Feng, G.; Mareque-Rivas, J. C.; Williams, N. H. *Chem. Commun.* **2006**, 1845–1847.
- (9) Yashiro, M.; Kaneiwa, H.; Onaka, K.; Komiyama, M. *Dalton Trans.* **2004**, 605–610.
- (10) Iranzo, O.; Elmer, T.; Richard, J. P.; Morrow, J. R. *Inorg. Chem.* **2003**, *42*, 7737–7746.

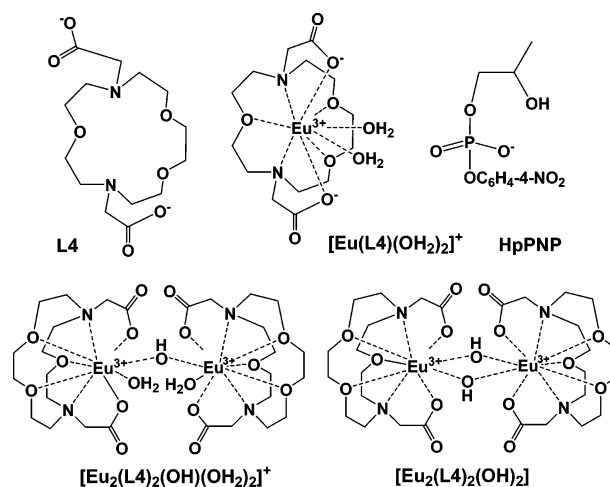


because of stronger interactions between the cationic catalyst and the anionic substrate.¹¹

A step toward the design of more powerful catalysts of RNA cleavage is to explore catalysis by dinuclear Ln(III) complexes, which may be more effective than complexes of Zn(II) because of their stronger electrostatic interactions with anionic phosphate ester substrates. There are few examples of Ln(III) dinuclear catalysts, and considerable difficulties will no doubt be encountered in preparing ligands that bind two Ln(III) ions and hold them in close proximity,^{12–18} as is required for *cooperative* stabilization of the transition state for RNA cleavage.^{5,10} Most reported examples of active dinuclear Ln(III) catalysts of RNA cleavage utilize weakly bound ligands.^{19–23} This approach favors aggregation and precipitation of the metal ion, complicating the characterization of these complexes in solution.^{24–27} In this category are methoxide-bridged dinuclear lanthanum(III) complexes that are effective catalysts for the cleavage of RNA analogs in methanol, yet have a complex distribution of catalytically active species.²⁸ In aqueous solution, a dimeric La(III) complex that is stabilized by interaction with buffer and hydroxide ligands is an effective catalyst for the cleavage of the dinucleoside ApA²⁹ but is kinetically unstable and precipitates from solution over time. The high activity of these catalysts is encouraging and has prompted the present

study of more complex ligands that react with lanthanides to form complexes of greater structural integrity.

Scheme 1



The septadentate L4 ligand (Scheme 1) forms a stable Eu(III) complex at neutral pH, which includes two water molecules most likely held in a *cis* geometry ($[Eu(L4)(OH_2)_2]^+$).^{30–32} Eu(III) excitation luminescence experiments have shown that at pH 10 the complex is converted to a species with either two hydroxide ligands or one water ligand,³⁰ however, the activity of these complexes as catalysts for the cleavage of RNA analogs has not been determined. We report here the results of a detailed study of the solution chemistry of Eu(III) complexes of L4 by pH–potentiometric titration and ¹H NMR spectroscopy. Our data show that the mononuclear complex $[Eu(L4)(OH_2)_2]^+$ dimerizes to form $[Eu_2(L4)_2(OH)(H_2O)_2]^+$ at pH > 8 in a reaction that consumes one mole of hydroxide ion per dimeric complex. The dependence of the apparent second-order rate constants for $[Eu(L4)(OH_2)_2]^+$ -catalyzed cleavage of the small RNA analog HpPNP on pH and on the concentrations of the metal ion complexes under the specified reaction conditions shows that catalysis is mainly due to the monomeric complex at low pH where this is the dominant complex and by the dimeric, hydroxide-ion-bridged complex at and above pH 9.0 where it begins to predominate. These data show that the expected large catalytic activity of these Eu(III) complexes is strongly attenuated by chelation to the ligand donors used here, in contrast to complexes that have more available coordination sites or weaker donor ligands. They provide insight into the problematic nature of the *de novo* synthesis of metal ion catalysts of RNA cleavage and suggest desirable properties for a good catalyst.

Experimental Section

All of the aqueous solutions were prepared with Millipore MILLI-Q purified water. The ligand 1,7-diaza-4,10,13-trioxacyclo-pentadecane-*N,N'*-diacetic acid (H₂L4) was prepared as the

- (11) Liu, C. T.; Neverov, A. A.; Brown, R. S. *Inorg. Chem.* **2007**, *46*, 1778–1788.
 (12) Chang, C. A.; Wu, B. H.; Kuan, B. Y. *Inorg. Chem.* **2005**, *44*, 6646–6654.
 (13) Komiyama, M.; Takeda, N.; Shigekawa, H. *Chem. Commun.* **1999**, 1443–1451.
 (14) Yashiro, M.; Ishikubo, A.; Komiyama, M. *J. Biochem.* **1996**, *120*, 1067–1069.
 (15) Jurek, P. E.; Jurek, A. M.; Martell, A. E. *Inorg. Chem.* **2000**, *39*, 1016–1020.
 (16) Jurek, P. E.; Martell, A. E. *Chem. Commun.* **1999**, 1609–1610.
 (17) Branum, M. E.; Que, L., Jr. *J. Biol. Inorg. Chem.* **1999**, *4*, 593–600.
 (18) Branum, M. E.; Tipton, A. K.; Zhu, S.; Que, L., Jr. *J. Am. Chem. Soc.* **2001**, *123*, 1898–1904.
 (19) Aguilar-Pérez, F.; Gómez-Tagle, P.; Collado-Fregoso, E.; Yatsimirsky, A. K. *Inorg. Chem.* **2006**, *45*, 9502–9517.
 (20) Calderón, A.; Yatsimirsky, A. K. *Inorg. Chim. Acta.* **2004**, *357*, 3483–3492.
 (21) Gómez-Tagle, P.; Yatsimirsky, A. K. *Inorg. Chem.* **2001**, *40*, 3786–3796.
 (22) Gómez-Tagle, P.; Yatsimirsky, A. K. *J. Chem. Soc., Dalton Trans.* **2001**, 2663–2670.
 (23) Medrano, F.; Calderón, A.; Yatsimirsky, A. K. *Chem. Commun.* **2003**, 1968–1970.
 (24) Wang, R.; Carducci, M. D.; Zheng, Z. *Inorg. Chem.* **2000**, *39*, 1836–1837.
 (25) Wang, R.; Liu, H.; Carducci, M. D.; Jin, T.; Zheng, C.; Zheng, Z. *Inorg. Chem.* **2001**, *40*, 2743–2750.
 (26) Wang, R.; Selby, H. D.; Liu, H.; Carducci, M. D.; Jin, T.; Zheng, Z.; Anthis, J. W.; Staples, R. J. *Inorg. Chem.* **2002**, *41*, 278–286.
 (27) Zheng, Z. *Chem. Commun.* **2001**, 2521–2529.
 (28) Tsang, J. S. W.; Neverov, A. A.; Brown, R. S. *J. Am. Chem. Soc.* **2003**, *125*, 1559–1566.
 (29) Hurst, P.; Takasaki, B. K.; Chin, J. *J. Am. Chem. Soc.* **1996**, *118*, 9982–9983.

- (30) Holz, R. C.; Klakamp, S. L.; Chang, C. A.; Horrocks, W. D., Jr. *Inorg. Chem.* **1990**, *29*, 2651–2658.
 (31) Chang, C. A.; Garg, B. S.; Manchanda, V. K.; Ochaya, V. O.; Sekhar, V. C. *Inorg. Chim. Acta.* **1986**, *115*, 101–106.
 (32) Chang, C. A.; Ochaya, V. O. *Inorg. Chem.* **1986**, *25*, 355–358.

hydrobromide salt ($[\text{H}_4\text{L4}](\text{Br})_2$) according to a modification of a literature procedure.³² The ligand obtained as the crude reaction product was dissolved in ethanol, concentrated HBr in water was slowly added with stirring, and the resulting precipitate was collected and washed with ethanol to give pure product. The barium salt of 2-hydroxypropyl-4-nitrophenyl phosphate (HpPNP) was prepared by a published procedure.³³ Aqueous stock solutions (20.0 mM) of $[\text{H}_4\text{L4}](\text{Br})_2$ were prepared, and the concentration was determined by ^1H NMR using *p*-toluenesulfonic acid as an internal standard. Stock solutions of the lanthanide(III) salts (20.0 mM) were standardized by EDTA titration with an Arsenazo indicator.³⁴ The following buffers were used to maintain constant pH in kinetic studies of the cleavage of HpPNP: piperazine-*N,N'*-bis(2-ethanesulfonic acid) (PIPES, pH 6.7–7.2); *N*-(2-hydroxyethyl)piperazine-*N'*-(2-ethanesulfonic acid) (HEPES, pH 7.5–7.75); *N*-(2-hydroxyethyl)piperazine-*N'*-(3-propanesulfonic acid) (EPPS, pH 8.0–8.5), 2-(*N*-cyclohexylamino)ethanesulfonic acid (CHES, pH 9.0–9.4); and 3-(cyclohexylamino)-1-propanesulfonic acid (CAPS, pH 10.0–10.5).

An Orion Research Digital Ionalyzer 501 pH meter equipped with a ThermoOrion Ross Combination pH Electrode model 8115BN was used for all of the pH measurements. All of the kinetic experiments were carried out on either a Bio-Tek Instruments UVIKON-XL spectrophotometer or a Kontron Instruments Uvikon 930 spectrophotometer, both of which were equipped with a thermostatted cell transport compartment. ^1H NMR (500 MHz) spectra were recorded on a Varian Inova 500 spectrometer. Chemical shifts are reported as parts per million (ppm) downfield from tetramethylsilane (TMS). All of the ^1H NMR spectra were recorded at ambient temperature (20–22 °C) unless indicated otherwise. ^{31}P NMR spectra were recorded at 161.9 MHz on a Varian Inova 400 spectrometer, with ^{31}P NMR shifts reported in ppm with respect to an 85% phosphoric acid external reference.

pH–Potentiometric Titrations. Standard solutions of buffer from Fisher Chemicals at pH 4.00 (± 0.01), 7.00 (± 0.01), and 10.00 (± 0.02) were used to calibrate the pH meter. All of the solutions were prepared with freshly boiled Millipore MILLI-Q water that had been cooled under argon. Solutions of KOH were prepared by dilution of a concentrated solution from a J. T. Baker Dilut-It ampule and standardized by titration of potassium hydrogen phthalate. The complexes were prepared by combining EuCl_3 and L4 in a 1:1 ratio to give final concentrations of 1.00 mM ligand and Eu^{3+} . The pH titrations were at 25.0 °C under argon at a constant ionic strength of 0.10 M (KCl). The stability and protonation constants for the $\text{Eu(III)}\text{--L4}$ complexes were determined from the collected titration data using (1) Literature acidity constants for protonation of L4,³² (2) $\text{Log } K_w = \text{log } [\text{H}^+][\text{OH}^-] = 10^{-13.78}$ at 25.0 °C and $I = 0.10$ M KCl.³⁵ The pH meter provides a measure of proton activity ($\text{pH} = -\text{log } a_{\text{H}^+}$) rather than $[\text{H}^+]$ ($\text{p}[\text{H}] = -\text{log } [\text{H}^+]$, where $a_{\text{H}^+} = \gamma_{\text{H}^+}[\text{H}^+]$). Therefore, the stability and protonation constants calculated from these titration data are not true thermodynamic constants but will be close to these because $\gamma_{\text{H}^+} \approx 1$ in a dilute aqueous solution.

The titration data were fit by a nonlinear least-squares analysis to Scheme 1a in the Supporting Information using HYPERQUAD 2000 Version 2.1 NT. This least-squares refinement was carried out to obtain the best combination of acceptable values of the

weighted error in the residuals σ^2 ($\sigma^2 \leq 9$ or $\sigma^2 \leq 3$) and the goodness of fit statistic χ^2 at 95% confidence ($\chi^2 \leq 12.6$).

^1H NMR Spectroscopy. ^1H NMR spectra were recorded at 500 MHz in D_2O at a constant ionic strength of 0.10 M (KCl) for solutions that were 1.05 mM in L4 and 1.00 mM in EuCl_3 . The pH of the solutions was adjusted with dilute KOD. The solutions were typically 80–90% D_2O . Therefore, the pH meter reading pH_{obs} was corrected to give pD using eq 1 where α is the atom fraction of deuterium in the solvent.³⁶

$$\text{pD} = \text{pH}_{\text{obs}} + 0.3314\alpha + 0.0766\alpha^2 \quad (1)$$

Kinetic Experiments. The transesterification of HpPNP at 25.0 °C was followed by monitoring the increase in absorbance at 400 nm due to the formation of 4-nitrophenolate anion. The solutions were prepared by mixing EuCl_3 and L4 in a 1.0:1.1 ratio with 20.0 mM of a suitable buffer at $I = 0.10$ M (KCl) to give a final Eu(III) concentration between 0.10 and 1.5 mM. Dilute KOH or HCl was then added to obtain the desired pH. The solution was incubated at 25.0 °C, and HpPNP was added to give a final concentration of 0.0375 mM. The pH was measured at the conclusion of each reaction and was generally within 0.04 pH units of the initial value. The reaction of HpPNP was followed for at least three half-lives and an endpoint determined after 10 half-lives was used when the concentration of Eu(III) in solution was between 0.75 and 1.5 mM. The transesterification was followed for at least one half-life at lower Eu(III) concentrations of between 0.10 and 0.50 mM. In the case of the slowest reactions, the endpoint was obtained by incubation of the reaction solution at 60 °C. The pseudo-first-order rate constants k_{obs} (s^{-1}) for these reactions were determined as the slopes of semilogarithmic plots of reaction progress ($A_\infty - A_t$) against time, where A_t is the observed absorbance at 400 nm and A_∞ is the final absorbance at the end of the reaction. For reactions at pH 6.70–9.00, the values of k_{obs} were found to be reproducible to $\pm 5\%$. The background rate constants k_0 (s^{-1}) for the transesterification of HpPNP in the absence of the catalyst were determined for several pH values by the method of initial rates.

Results

The formation and stability of complexes between Eu(III) and L4 were examined at 25.0 °C and $I = 0.10$ M (KCl) by quantifying the acid released upon mixing equimolar concentrations of Eu(III) and fully protonated L4. Figure 1 shows the results of a typical pH–potentiometric titration of a mixture of 1.00 mM L4 and 1.00 mM Eu(III) . Two molar equivalents of hydroxide ion are consumed between pH 4 and 6 as a result of the loss of protons from the ligand that occurs upon the binding of Eu(III) to L4, to form $[\text{Eu}(\text{L4})(\text{OH}_2)_2]^+$. Interestingly, the concentration of hydroxide ion required to bring the pH to 11 is greater than that required to ionize the solvent water. This is shown by the inset to Figure S1 in the Supporting Information, which corrects for the ionization of water. These data show that approximately 0.5 equiv of hydroxide ion are consumed by Eu(L4) complexes as the pH is increased from pH 7 to 10 and that an additional 0.5 equiv of hydroxide ion are consumed as the pH is increased to 11.

The results of laser-induced Eu(III) luminescence studies on $[\text{Eu}(\text{L4})(\text{OH}_2)_2]^+$ at pH 6.0 yield the straightforward

(33) Brown, D. M.; Usher, D. A. *J. Chem. Soc.* **1965**, 6558–6564.

(34) Fritz, J. S.; Oliver, R. T.; Pietrzyk, D. J. *Anal. Chem.* **1958**, *30*, 1111–1114.

(35) Sweeton, F. H.; Mesmer, R. E.; Baes, C. F., Jr. *J. Solution Chem.* **1974**, *3*, 191–214.

(36) Salomaa, P.; Schaleger, L. L.; Long, F. A. *J. Am. Chem. Soc.* **1964**, *86*, 1–7.

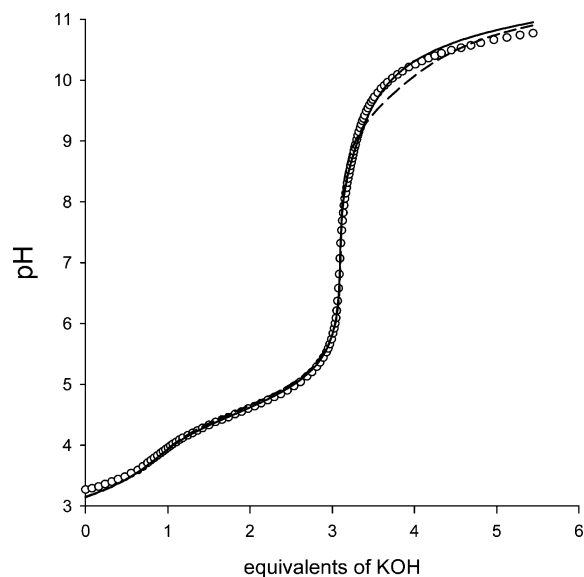


Figure 1. Comparison of the observed consumption of KOH during the titration of a mixture of 1.0 mM Eu(III) and 1.0 mM L4, with the titration curves calculated for the formation of a monomeric complex between Eu(III) and L4 that loses a proton at high pH (dashed line in Scheme S1b; $\chi^2 = 15.7$, $\sigma = 5.14$) and the curve calculated for the dimerization of the monomeric complex that is accompanied by the loss of a proton from the dimeric species (solid line, calculated for Scheme S1a; $\chi^2 = 6.56$, $\sigma = 2.65$).

conclusion that this is a 1:1 metal–ligand complex with complete coordination of all of the macrocyclic chelating atoms and two coordinated water molecules to give a nine-coordinate Eu(III) complex as shown in Scheme 1.³⁰ The changes in the excitation luminescence spectrum of $[\text{Eu}(\text{L4})(\text{OH}_2)_2]^+$ and luminescence lifetimes that are observed as the pH was increased from 6 to 10 are consistent with the ionization of these coordinated water molecules, but the consequences for the speciation of the complex were not fully rationalized.³⁰ By pH–potentiometric methods, we observe the consumption of ca. 0.5 equiv of hydroxide ion as the pH is increased from 7 to 10 during titration of a mixture of 1.0 mM L4 and Eu(III). This is consistent with formation of a dimeric complex that is coupled to the loss of a proton to give $[\text{Eu}_2(\text{L4})_2(\text{OH})(\text{H}_2\text{O})_2]^+$ (K_D , Scheme 2). For this species, we assume that one water ligand is lost and that each Eu(III) center is nine-coordinate. The additional consumption of hydroxide ions at high pH is consistent with ionization of the dimeric complex to form $[\text{Eu}_2(\text{L4})_2(\text{OH})_2]$ ($(K_a)_D$, Scheme 2). Alternatively, we would expect a single proton to be consumed upon ionization of water bound to the monomeric complex. The dashed and solid lines in Figure 1 show, respectively, the poor fit of the experimental data to a simple model for ionization of a monomeric complex and the better fit of the data to Scheme 2. Values of $\log K_D = 7.5$ and $p(K_a)_D = 10.7$ were calculated from the fit of the experimental data to Scheme 2 (Supporting Information Scheme S1).

The data from the potentiometric titrations were used to construct a speciation diagram (Figure 2). This diagram shows that $[\text{Eu}(\text{L4})(\text{OH}_2)_2]^+$ is the dominant form of the catalyst between pH 6 and 8 and that the dimer $[\text{Eu}_2(\text{L4})_2(\text{OH})(\text{H}_2\text{O})_2]^+$ begins to accumulate at $\text{pH} > 8$.

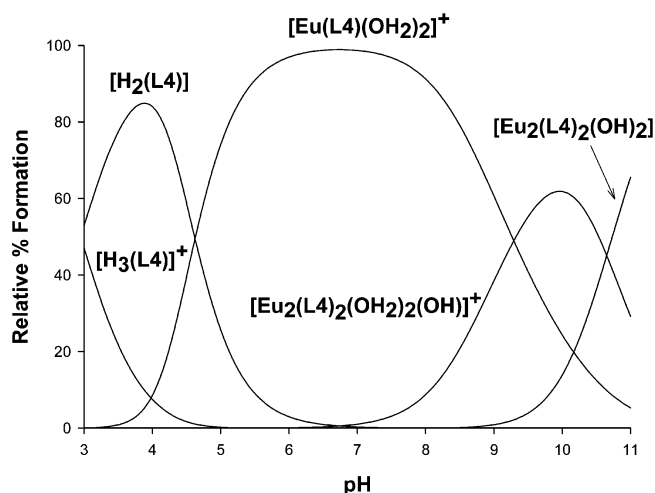
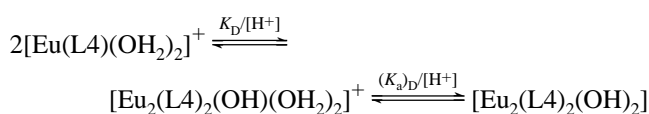


Figure 2. Change with increasing pH, in the relative concentrations of complexes between Eu(III) and L4, in a solution that contains an initial 1.0 mM concentration of EuCl_3 and L4.

Scheme 2



¹H NMR spectra (Figure 3) were obtained in D_2O at several pD values for a solution of 1.00 mM EuCl_3 and 1.05 mM L4 ($I = 0.10 \text{ M}$ (KCl)). These conditions are similar to those used for potentiometric titrations in H_2O . We are not able to present a full assignment of the resonances for the spectra in Figure 3 (Scheme S2 in the Supporting Information). However, the changes in these spectra that occur with increasing pD provide direct evidence of the formation of the dimeric complexes that were proposed to rationalize the data from the potentiometric titration shown in Figure 1.

The ¹H NMR spectra determined at pD 6.4 and 7.4 show 10 peaks between +4 and –10 ppm, some of which are very broad or consist of two or more overlapping resonances. Increasing the pD to 10.37 results in a decrease in the intensity of the peaks observed at low pD. These are replaced by a set of 11 new peaks that appear over a broader chemical-shift range of +13 to –15 ppm. Both the replacement of old resonances by new resonances at high pD and the larger chemical-shift dispersion of these new resonances are consistent with the conversion of a monomeric complex to a dimer. Ten of the 11 peaks show a relative area of 1.0 and the eleventh has an area of 2.0. The total relative area of 12.0 obtained from the high pD spectra is equal to the expected number of distinct macrocyclic proton environments present in $[\text{Eu}_2(\text{L4})_2(\text{OH})(\text{H}_2\text{O})_2]^+$ (Supporting Information, Scheme S2). Signals for the free ligand, which is present in 5% excess over EuCl_3 , are observed at both high and low pH; and, several small sharp resonances are observed in the ¹H NMR spectra determined at alkaline pH that are assigned to a complex between Ca(II) and L4 (Supporting Information, Figures S3 and S4). The intensity of these signals suggests that L4 was present in ca. 5% excess concentration over Eu(III).

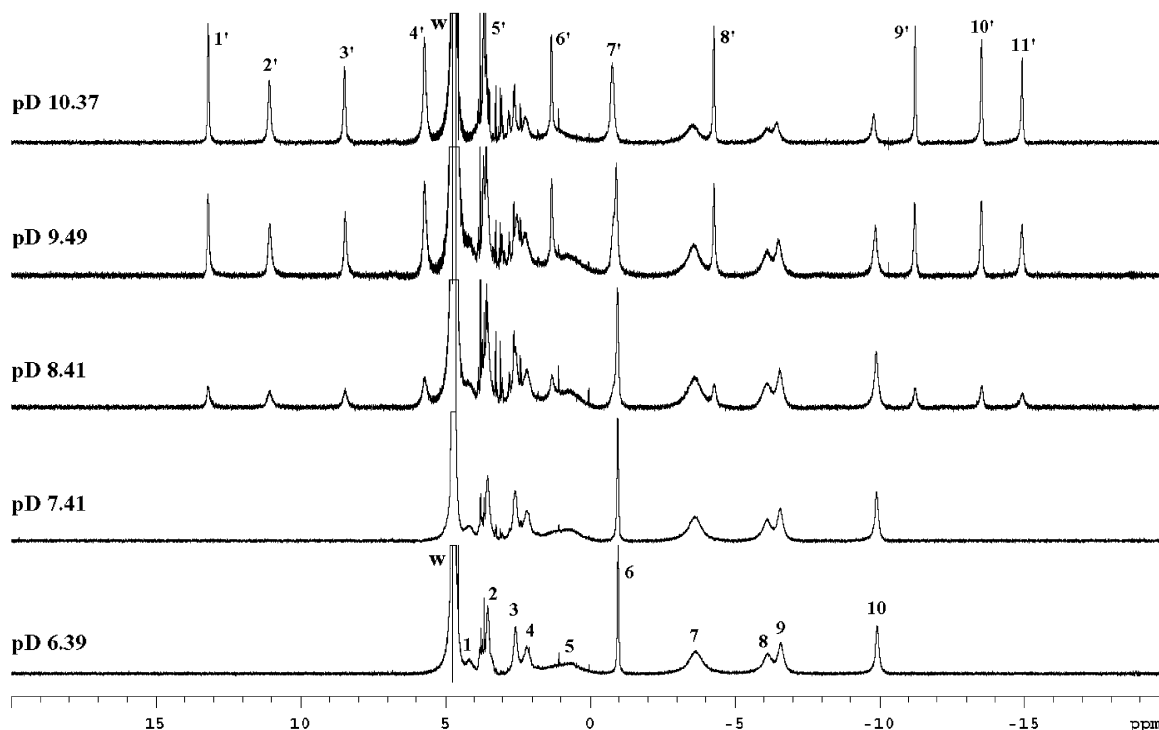


Figure 3. ^1H NMR spectra in D_2O of solutions containing $[\text{EuCl}_3] = 1.00 \text{ mM}$, $[\text{L4}] = 1.05 \text{ mM}$ with $I = 0.10 \text{ M}$ (KCl). The peak labeled w is the resonance for HDO. The ratio of the areas for peaks centered at -0.96 ppm (peak 6), -3.63 ppm (peak 7), -6.13 and -6.57 ppm (peaks 8 and 9), and -9.91 ppm (peak 10) is 1:2:2:1, respectively, and the peaks at 2.57 , 2.18 , and 0.75 ppm (peaks 3, 4, and 5) sum to a relative area of about 4. The 11 new peaks, which appear at high pH, show relative areas of 1 with the exception of the peak 4', which has a relative area of 2. The sharp peaks that appear between 1 and 6 ppm are shown in greater detail in Figure S3 of the Supporting Information.

Table 1. Observed First-Order Rate Constants for the Cleavage of HpPNP in Solutions that Contain a 1.0:1.1 Ratio of Eu(III) and L4 at 25°C and $I = 0.10$ (KCl)

pH ^b / [Eu(III)]	$k_{\text{obsd}}/10^{-5} \text{ s}^{-1} \text{ }^a$										
	0.00	0.10 mM	0.20 mM	0.25 mM	0.30 mM	0.40 mM	0.51 mM	0.74 mM	1.00 mM	1.25 mM	1.50 mM
6.70								0.093	0.12	0.16	0.18
7.00							0.13	0.20	0.28	0.36	0.40
7.50	0.0084	0.083	0.16	0.20	0.24	0.32	0.40	0.58	0.75	0.94	1.1
7.75	0.010	0.12		0.29	0.36	0.49	0.54	0.90	1.2	1.3	1.8
8.00	0.015	0.16	0.34	0.43	0.51	0.71	0.86	1.3	1.7	2.2	2.7
8.25	0.023	0.20	0.42	0.48	0.61	0.99	1.5	2.3	3.2	3.4	4.4
8.50	0.043	0.20	0.43	0.61	0.90	1.1	1.6	2.9	4.7	6.0	7.8
9.00	0.13	0.31	0.76	1.2	1.6	3.6	4.6	11	15	21	29

^a Observed first-order rate constant determined by monitoring the formation of nitrophenolate anion at 400 nm. ^b The pH is maintained by 20 mM of the appropriate buffer (Experimental Section).

Transesterification of 2-hydroxypropyl-4-nitrophenyl phosphate (HpPNP) catalyzed by Eu(III) complexes of L4 was followed by monitoring the increase in absorbance at 400 nm due to the formation of 4-nitrophenolate anion. It was shown by ^{31}P NMR that the cyclic phosphate diester is the sole phosphorus-containing product of the cleavage reaction in the presence of the $[\text{Eu}(\text{L4})(\text{OH}_2)_2]^+$ catalyst (Figure S5). Pseudo-first-order rate constants ($k_{\text{obsd}}, \text{s}^{-1}$) for the cleavage of HpPNP were determined over a wide range of catalyst concentrations and pH and are reported in Table 1. These observed rate constants increase by ca. 300-fold as the pH is increased from 6.7 to 9.0, and the concentration of Eu(III) is increased from 0.10 to 1.50 mM for reactions in the presence of a 10% excess concentration of the ligand L4. The second-order rate constant for the reaction catalyzed by hydroxide ion, $k_{\text{HO}} = 0.090 \text{ M}^{-1} \text{ s}^{-1}$, calculated from rate constants for the reaction in the absence of the Eu(III)

catalyst, is in acceptable agreement with the value of $0.099 \text{ M}^{-1} \text{ s}^{-1}$ from earlier work.³⁷

The Eu(III)-catalyzed cleavage reactions are first order in $[\text{Eu}(\text{III})] = [\text{Eu}(\text{L4})(\text{OH}_2)_2]^+$ for reactions at pH 6.70, 7.00, and 7.50 (Figure 4 and Table 1). The apparent second-order rate constants ($k_{\text{Mon,app}}$) for the $[\text{Eu}(\text{L4})(\text{OH}_2)_2]^+$ -catalyzed reactions, calculated as the slopes of these plots of data obtained at the three lowest pH values are reported in Table 2.

Figure 4 shows the plot of $k'_{\text{obsd}} = (k_{\text{obsd}} - k_0)$, where k_0 is the observed rate constant determined for the reaction in the absence of catalyst, against the total concentration of Eu(III) for reactions in solutions containing a 1.0:1.1 molar ratio of added Eu(III) and L4. This figure includes data for

(37) Yang, M.-Y.; Richard, J. P.; Morrow, J. R. *Chem. Commun.* **2003**, 2832–2833.

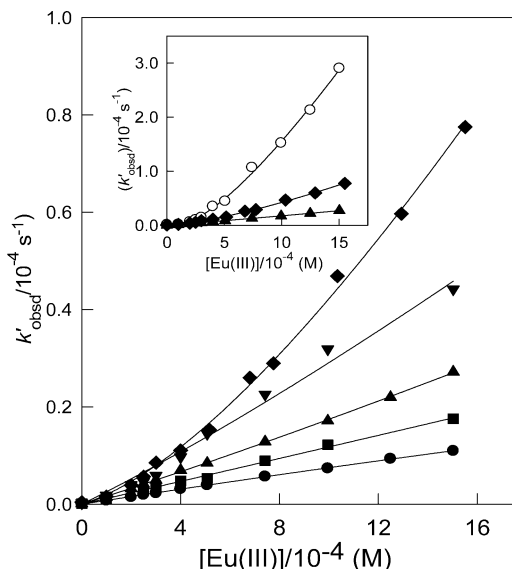


Figure 4. Increase in k'_{obsd} for the cleavage of HpPnP with increasing concentrations of Eu(III) in a solution that contains [Eu(III)] and [L4] in a ratio of 1.0:1.1. The figure shows data for reactions at increasing pH. The y axis for the inset has been enlarged to show data for reactions at pH 9.0, where there is a ca. 200-fold increase in k_{obsd} with increasing catalyst concentration. Key: pH 7.50, (●); pH 7.75, (■); pH 8.00, (▲); pH 8.25, (▼); pH 8.50, (▲); pH 9.0 (○).

Table 2. Apparent Second-Order Rate Constants for Transesterification of HpPnP Catalyzed by $[\text{Eu}(\text{L4})(\text{OH}_2)_2]^+$ and $[\text{Eu}_2(\text{L4})_2(\text{OH})(\text{OH}_2)_2]^+$ at 25.0 °C, $I = 0.10 \text{ M}$ (KCl)^{a,b}

pH	$[\text{Eu}(\text{L4})(\text{OH}_2)_2]^+$ $(k_{\text{Mon}})_{\text{app}}/10^{-2} (\text{M}^{-1} \text{s}^{-1})$	$[\text{Eu}_2(\text{L4})_2(\text{OH})(\text{OH}_2)_2]^+$ $(k_{\text{Di}})_{\text{app}}/10^{-2} (\text{M}^{-1} \text{s}^{-1})$
6.7	0.13 ± 0.01^c	
7.0	0.28 ± 0.045^c	
7.5	0.77 ± 0.033^c	
7.75 ^d	1.2 ± 0.05	2.6 ± 1.54
8.0 ^d	1.6 ± 0.02	6.3 ± 0.40
8.25 ^d	2.5 ± 0.30	11 ± 0.30
8.5 ^d	1.6 ± 0.20	28 ± 0.1
9.0		81 ± 0.1^e

^a The pH is maintained by 20 mM of the appropriate buffer (Experimental Section). ^b The quoted errors are standard deviations from the fits to the appropriate kinetic equation. ^c The slope of a plot of k'_{obsd} against $[[\text{Eu}(\text{L4})]_{\text{T}}] = [[\text{Eu}(\text{L4})(\text{OH}_2)_2]^+]$. ^d Obtained from the fits of the kinetic data from Figure 4 to eq 2, using the expressions in eq 2a and 2c for $[[\text{Eu}(\text{L4})(\text{OH}_2)_2]^+]$ and 2b and 2c for $[[\text{Eu}_2(\text{L4})_2(\text{OH})(\text{H}_2\text{O})_2]^+]$ and $K_{\text{D}} = 10^{7.5}$ (Scheme 2). ^e The slope of a plot of k'_{obsd} against $[[\text{Eu}_2(\text{L4})_2(\text{OH})(\text{H}_2\text{O})_2]^+]$ (Figure 5).

reactions at pH 7.5 where k_{obsd} for the cleavage of HpPnP is cleanly first-order in $[[\text{Eu}(\text{L4})(\text{OH}_2)_2]^+]$. The increasing curvature observed in the plots for reactions at pH > 7.5 provides evidence that Eu(III)-catalyzed phosphate diester cleavage is kinetically bimolecular in Eu(III). Figure 5 shows a plot of k'_{obsd} against the concentration of the dimeric complex $[\text{Eu}_2(\text{L4})_2(\text{OH})(\text{OH}_2)_2]^+$ calculated from the equilibrium constants determined by potentiometric titration for reactions at pH 9, where there are roughly equal concentrations of the monomeric and dimeric complexes (Figure 2). This linear plot provides strong evidence that catalysis is mainly due to dimeric $[\text{Eu}_2(\text{L4})_2(\text{OH})(\text{OH}_2)_2]^+$, implying that the dimer at pH 9 must be more reactive than the monomer. The slope of the linear portion of the plot shown in Figure 5 is reported in Table 2 as the apparent second-order rate

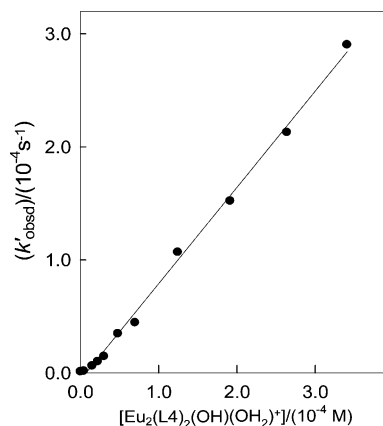


Figure 5. Increase in k'_{obsd} for the cleavage of HpPnP with increasing concentrations of the dimeric complex $[\text{Eu}_2(\text{L4})_2(\text{OH})(\text{OH}_2)_2]^+$.

constant k_{Di} for catalysis of the reaction by $[\text{Eu}_2(\text{L4})_2(\text{OH})(\text{OH}_2)_2]^+$ at pH 9.0.

The increasing deviation from a linear dependence of k'_{obsd} on Eu(III) (Figure 4) observed for reactions as the pH is increased from 7.75 to 8.5 provides evidence that the dimer $[\text{Eu}_2(\text{L4})_2(\text{OH})(\text{OH}_2)_2]^+$ is a good catalyst for cleavage of HpPnP at pH values where the monomer is the major complex (Figure 2). The data at an intermediate pH were fit to eq 2 using (i) The expressions in eqs 2a and 2c to relate the concentration of $[\text{Eu}(\text{L4})(\text{OH}_2)_2]^+$ to $[\text{Eu}(\text{L4})]_{\text{T}}$, where $[[\text{Eu}(\text{L4})]_{\text{T}}] = [[\text{Eu}(\text{L4})(\text{OH}_2)_2]^+] + 2[[\text{Eu}_2(\text{L4})_2(\text{OH})(\text{OH}_2)_2]^+]$, (ii) the expressions in eqs 2b and 2c to relate the concentration of the dimeric complex $[\text{Eu}_2(\text{L4})_2(\text{OH})(\text{H}_2\text{O})_2]^+$ to $[\text{Eu}(\text{L4})]_{\text{T}}^+$, and (iii) a value of $K_{\text{D}} = 10^{7.5}$, determined by potentiometric titration. The values of the apparent second-order rate constants $(k_{\text{Mon}})_{\text{app}}$ and $(k_{\text{Di}})_{\text{app}}$ obtained from the fits of the kinetic data to eq 2 are reported in Table 2.

$$k'_o = k_{\text{Mon}}[[\text{Eu}(\text{L4})(\text{OH})(\text{OH}_2)_2]^+] + k_{\text{Di}}[[\text{Eu}_2(\text{L4})_2(\text{HO})(\text{OH}_2)_2]^+] \quad (2)$$

$$[\text{Eu}(\text{L4})(\text{OH}_2)_2]^+ = \left[\frac{-[\text{H}^+] + \alpha}{4K_{\text{D}}} \right] \quad (2a)$$

$$[\text{Eu}_2(\text{L4})_2(\text{HO})(\text{OH}_2)_2]^+ = \left[\frac{[\text{H}^+] + 4K_{\text{D}}[\text{Eu}(\text{L4})]_{\text{T}} - \alpha}{8K_{\text{D}}} \right] \quad (2b)$$

$$\alpha = \sqrt{[\text{H}^+]^2 + 8K_{\text{D}}[\text{Eu}(\text{L4})]_{\text{T}}[\text{H}^+]} \quad (2c)$$

Discussion

Complexes Between Eu(III) and L4. The complex between L4 and Eu(III) ($[\text{Eu}(\text{L4})(\text{OH}_2)_2]^+$) that forms at neutral pH has been characterized in earlier work using Eu(III) direct-excitation luminescence and pH-potentiometric titrations under a more limited set of conditions than those examined here.^{30–32} Our pH-potentiometric titration studies at pH 7–10 show that Eu(III) and L4 combine at neutral pH for the formation of $[\text{Eu}(\text{L4})(\text{OH}_2)_2]^+$ and they are consistent with the combination of two $[\text{Eu}(\text{L4})(\text{OH}_2)_2]^+$ at

higher pH to form a dimeric complex $[\text{Eu}_2(\text{L4})_2(\text{OH})(\text{H}_2\text{O})_2]^+$ that results in the release of one mol/ HO^- per mol/dimer formed. We propose that dimerization proceeds by the ionization of a metal-bound water of $[\text{Eu}(\text{L4})(\text{OH}_2)_2]^+$ to form $[\text{Eu}(\text{L4})(\text{OH})(\text{OH}_2)]$ and that this combines with a second $[\text{Eu}(\text{L4})(\text{OH}_2)_2]^+$ to afford the observed dimer (Scheme 2). This pH-dependent conversion of $[\text{Eu}(\text{L4})(\text{OH}_2)_2]^+$ to $[\text{Eu}_2(\text{L4})_2(\text{OH})(\text{H}_2\text{O})_2]^+$ provides a simple explanation for (a) the large changes in the ^1H NMR chemical shifts of Eu(III) L4 complex protons observed as the pD of a 1.00 mM solution of EuCl_3 and L4 at $I = 0.10$ M (KCl) is increased from 6.4 to 10.4, and (b) the observed first-order rate constants determined for the cleavage of HpPNP in the presence of increasing $[\text{Eu}(\text{III})] = [\text{L4}]$, as discussed below.

Potentiometric titration also provides evidence for the loss of a proton from $[\text{Eu}_2(\text{L4})_2(\text{OH})(\text{H}_2\text{O})_2]^+$ with a $\text{p}K_a$ of 10.7 to form $[\text{Eu}_2(\text{L4})_2(\text{OH})_2]$. We suggest that the two Eu(III) centers in $[\text{Eu}_2(\text{L4})_2(\text{OH})_2]$ are linked by a pair of bridging cis-hydroxide ligands, similar to that observed for structurally characterized dinuclear lanthanide complexes with two bridged hydroxides.³⁸ We were unable to characterize the catalytic activity of this complex for the cleavage of HpPNP because the kinetic data at $\text{pH} > 9.00$ were not reproducible. In some cases, the slow formation of a precipitate was observed at high pH in buffered solutions, but this material was not characterized further.

pH-Dependence of the Catalytic Activity of Eu(III) Complexes. Figure 2 shows that the dominant form of the complex between L4 and Eu(III) changes from the monomer to the dimer over the pH range where the shape of the plots of k'_{obsd} for the cleavage of HpPNP against the concentration of $\text{Eu}(\text{III}) = [\text{Eu}(\text{L4})]_{\text{T}}$ changes from linear to curved upward (Figure 4). The kinetic data at the lowest and highest pH were fit to simple models for exclusive catalysis by the monomeric and dimeric complexes, respectively. The data at intermediate pH were fit to eq 2, which contains separate rate terms for catalysis by the monomeric $[\text{Eu}(\text{L4})(\text{OH}_2)_2]^+$ and the dimeric $[\text{Eu}_2(\text{L4})_2(\text{OH})(\text{H}_2\text{O})_2]^+$ complexes and using $K_{\text{D}} = 10^{7.5}$ (Scheme 2) determined by potentiometric titration for conversion of the monomer and dimer. The rate constants for the reactions catalyzed by these different species are reported in Table 2.

Figure 6 shows the logarithmic pH dependence of the apparent second-order rate constants for the cleavage of HpPNP catalyzed by the monomeric $(k_{\text{Mon}})_{\text{app}}$ and dimeric $(k_{\text{Di}})_{\text{app}}$ Eu(III) complexes. The values of $(k_{\text{Mon}})_{\text{app}}$ are first-order in $[\text{HO}^-]$ for reactions at $\text{pH} 6-8$, but a downward deflection in the pH rate profile is observed at the highest pH. The data for the monomer are consistent with a reaction whose rate is controlled by an ionizable group of $\text{p}K_a$ 8.0. This is similar to the $\text{p}K_a$ reported for several similar Ln(III) carboxylate complexes.^{31,39,40} The $\text{p}K_a$ for $[\text{Eu}(\text{L4})(\text{OH}_2)_2]^+$ calculated from these data is determined mainly

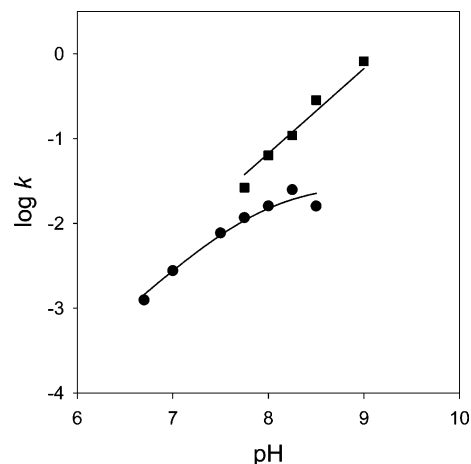
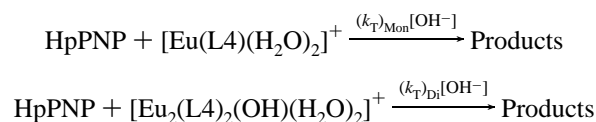


Figure 6. pH-Rate profiles for HpPNP cleavage catalyzed by $[\text{Eu}(\text{L4})(\text{OH}_2)_2]^+$ ($(k_{\text{Mon}})_{\text{app}}$, $\text{M}^{-1} \text{s}^{-1}$, ●) with data fit to equation S1 (in Supporting Information) and $[\text{Eu}_2(\text{L4})_2(\text{OH})(\text{H}_2\text{O})_2]^+$ ($(k_{\text{Di}})_{\text{app}}$, $\text{M}^{-1} \text{s}^{-1}$, ■).

by the value of the rate constant for reaction at $\text{pH} 8.50$, where the catalysis by the dimeric complex predominates. Consequently, there is a large uncertainty in the rate constant that controls the position of the downward break and in the $\text{p}K_a$ calculated from the data shown in Figure 6. Further, the ionized monomer was not detected by pH-potentiometric titration of solutions that contain 1 mM Eu(III) and L4. The concentration of the ionized monomer is reduced by its reaction with $[\text{Eu}(\text{L4})(\text{OH}_2)_2]^+$ to form $[\text{Eu}_2(\text{L4})_2(\text{OH})(\text{H}_2\text{O})_2]^+$ (Scheme 2). We conclude that the kinetic data provide evidence for partial ionization of $[\text{Eu}(\text{L4})(\text{OH}_2)_2]^+$ at $\text{pH} 8.5$ but that the $\text{p}K_a$ of this complex is probably greater than the value of 8.0 obtained from the fit of the kinetic data.

A value of $(k_{\text{T}})_{\text{Mon}} = 1.8 \times 10^4 \text{ M}^{-2} \text{ s}^{-1}$ was calculated as the apparent third-order rate constant for $[\text{Eu}(\text{L4})(\text{OH}_2)_2]^+$ -catalyzed cleavage of HpPNP (Scheme 3) using the values of $(k_{\text{Mon}})_{\text{app}}$ that show a first-order dependence on $[\text{HO}^-]$. The rate constants $(k_{\text{Di}})_{\text{app}}$ ($\text{M}^{-1} \text{s}^{-1}$) for the reaction catalyzed by the dimeric Eu(III) complex $[\text{Eu}_2(\text{L4})_2(\text{OH})(\text{H}_2\text{O})_2]^+$ are cleanly first-order in $[\text{HO}^-]$, and there is no significant accumulation of ionized dimeric complex $[\text{Eu}_2(\text{L4})_2(\text{OH})_2]$ ($\text{p}K_{\text{aD}} = 10.7$) at the highest pH used for these kinetic experiments (Figure 2). A value of $(k_{\text{T}})_{\text{Di}} = 4 \times 10^4 \text{ M}^{-2} \text{ s}^{-1}$ was calculated as the apparent third-order rate constant for $[\text{Eu}_2(\text{L4})_2(\text{OH})(\text{H}_2\text{O})_2]^+$ -catalyzed cleavage of HpPNP (Scheme 3) from the values of $(k_{\text{Di}})_{\text{app}}$ that are first order in $[\text{HO}^-]$.

Scheme 3



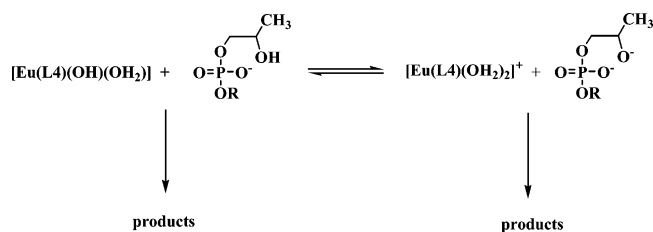
Reaction Mechanism. Previously, we have shown that the pH rate profiles (Figure 6) of apparent second-order rate constants for the catalysis of phosphate diester cleavage by Zn(II) complexes show a region at low pH where the rate constant increases linearly with increasing $[\text{HO}^-]$, a region

(38) Lisowski, J.; Starynowicz, P. *Inorg. Chem. Commun.* **2003**, 6, 593–597.

(39) Chang, C. A.; Chen, Y.-H.; Chen, H.-Y.; Shieh, F.-K. *J. Chem. Soc., Dalton Trans.* **1998**, 3243–3248.

(40) Wu, S. L.; Horrocks, W. D., Jr. *Anal. Chem.* **1996**, 68, 394–401.

Scheme 4



at high pH where the apparent rate constants are pH independent, and a downward break that correlates well with the pK_a of a water coordinated to the metal ion catalyst.^{1,4,37} The pH rate profiles of apparent second-order rate constants for the Eu(III) catalysts described in this work also show the region at neutral pH with a unit slope. There is evidence discussed above for a downward break at high pH for the reaction catalyzed by the monomeric complex but the larger number of catalytic species complicates our analysis of these data.

The linear dependence of the second-order rate constants for metal ion-catalyzed cleavage of HpPNP shows that a proton is lost on proceeding from the reactants in solution to the transition state for the reaction at neutral pH. This proton may be lost either from a catalyst-bound water (Scheme 4, left-hand side) or from the C-2 hydroxyl of substrate (Scheme 4, right-hand side) as shown here for the mononuclear complex.¹ These two reaction pathways are kinetically equivalent because they proceed through transition states of identical stoichiometry. The first pathway requires that there be proton transfer from the substrate to the catalyst upon proceeding to the transition state. This should lead to a primary solvent deuterium isotope effect. The absence of a primary solvent deuterium isotope effect on $[\text{Zn}_2(\text{L}1)(\text{OH}_2)]^{3+}$ -catalyzed cleavage of uridine-3'-4-nitrophenyl phosphate shows that there is no partial proton transfer from the substrate to the catalyst at the rate determining step for the catalyzed reaction. Instead, there is full proton transfer from the substrate to the catalyst to form the ionized substrate and protonated catalyst prior to the formation of the phosphorane transition state and cleavage of the phosphate diester.¹ As noted previously, proton transfer might occur between the free reactant and the catalyst in solution or between the substrate-catalyst complex,^{1,4} and these pathways are not readily distinguished.

The preferred mechanism for this reaction depends upon the balance between the transition-state stabilization from Brønsted acid-base catalysis obtained for the reaction where the proton is "in flight" at the transition state and the electrostatic stabilization of the transition state that is sacrificed when the negative charge at the substrate is neutralized by the transferred proton. Electrostatic considerations are dominant for $[\text{Zn}_2(\text{L}1)(\text{OH}_2)]^{3+}$ -catalyzed cleavage of HpPNP; and we have argued that this will generally be the case for the stabilization of the dianionic transition state for phosphate diester cleavage by interaction with cationic metal complexes such as $[\text{Eu}(\text{L}4)(\text{OH}_2)_2]^+$ and $[\text{Eu}_2(\text{L}4)_2(\text{OH})(\text{H}_2\text{O})_2]^+$.^{4,5}

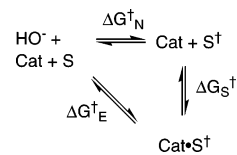
Table 3. Kinetic Parameters for the Cleavage of HpPNP Catalyzed by Mononuclear and Dinuclear Metal-Ion Complexes^a

Metal Ion Complex	k_T ($\text{M}^{-2}\text{s}^{-1}$) ^b	k_T/k_{HO} (M^{-1}) ^c	$\Delta\Delta G^\ddagger$ (kcal/mol) ^d
$[\text{Zn}_2(\text{L}1)(\text{OH}_2)]^{3+e}$	1.1×10^6	1.1×10^7	-9.6
$[\text{Cd}_2(\text{L}1)(\text{OH}_2)]^{3+f}$	4.0×10^5	4.0×10^6	-9.0
$[\text{Zn}(\text{L}2)(\text{OH}_2)]^{2+e}$	3.8×10^3	3.8×10^4	-6.2
$[\text{Eu}(\text{L}4)(\text{OH}_2)_2]^+g$	1.8×10^4	1.8×10^5	-7.1
$[\text{Eu}_2(\text{L}4)_2(\text{OH})(\text{H}_2\text{O})_2]^+g$	4×10^4	4.0×10^5	-7.6

^a For the reaction where there is a loss of a proton from the C-2 hydroxyl of HpPNP on proceeding from the reactant to transition state. ^b Rate constant that is defined by Scheme 3. ^c For reactions defined in Scheme 5. ^d Calculated using eq 3. ^e Ref 5. ^f Ref 6. ^g This work.

Specificity of Mononuclear and Dinuclear Zn(II) and Eu(III) Catalysts. The lines of the unit slope from Figure 6 define the apparent third-order rate constant for the hydroxide ion/metal complex catalyzed cleavage of HpPNP. These rate constants provide a measure of the specificity of different catalysts for the binding of the transition state for the cleavage reaction.^{1,36} This is illustrated by eq 3, derived for Scheme 5, which defines catalytic specificity as the Gibbs free energy associated with the binding of the transition state for specific base-catalyzed cleavage of HpPNP by different metal ion complexes.⁴¹ This binding energy was calculated from the ratio of the rate constants for (1) the apparent third-order rate constant k_T for the catalyzed reaction at low pH, where the catalyst exists mainly in the protonated form and (2) the second-order rate constant k_{HO} for the reaction catalyzed by the hydroxide ion. The transition-state binding energies calculated for the cleavage of HpPNP catalyzed by several mononuclear and dinuclear Zn(II), Cd(II), and Eu(III) catalysts are reported in Table 3.

Scheme 5



$$\Delta G_S^\ddagger = \Delta G_E^\ddagger - \Delta G_N^\ddagger = -RT \ln \left[\frac{k_T}{k_{\text{HO}}} \right] \quad (3)$$

The data in Table 3 shows the following.

(1) There is only a small difference in the stabilization of the transition state for specific-base-catalyzed cleavage of HpPNP by interaction with $[\text{Zn}(\text{L}2)(\text{OH}_2)]^{2+}$ compared with $[\text{Eu}(\text{L}4)(\text{OH}_2)_2]^+$. A larger difference might have been expected, given earlier observations that Eu(III) macrocyclic complexes with neutral amide or alcohol pendant groups have second-order rate constants at pH 7.4 that are 10–100-fold larger than the mononuclear Eu(III) complex reported here.^{42–45} The most likely explanation for the lack of a larger stabilization of the dianionic transition state by interaction with the Eu(III) complex is that the L4 macrocycle contains two strongly coordinating carboxylate groups that attenuate the Lewis acidity of $[\text{Eu}(\text{L}4)(\text{OH}_2)_2]^+$. Additionally, interactions with the macrocyclic ligand may interfere with binding

(41) Yatsimirsky, A. K. *Coord. Chem. Rev.* **2005**, *249*, 1997–2011.

of substrate to $[\text{Eu}(\text{L4})(\text{OH}_2)_2]^+$. However, this latter explanation is less likely because $[\text{Eu}(\text{L4})(\text{OH}_2)_2]^+$ has two coordination sites in cis geometry for interaction with the substrate and, in previous studies, this was shown to be sufficient to produce highly effective Ln(III) catalysts.⁴⁶

(2) There is only a small difference in the stabilization of the transition state for specific-base-catalyzed cleavage of HpPNP by interaction with $[\text{Eu}(\text{L4})(\text{OH}_2)_2]^+$ compared with $[\text{Eu}_2(\text{L4})_2(\text{OH})(\text{H}_2\text{O})_2]^+$. Similarly, small differences in catalytic activities were observed for a broad series of mono- and dinuclear Zn(II) catalysts (e.g., $[\text{Zn}(\text{L2})(\text{OH}_2)]^{2+}$ and $[\text{Zn}_2(\text{L3})(\text{OH}_2)]^{4+}$).¹⁰ Dinuclear complexes that do not have two metal ions positioned in close proximity for interaction with the transition-state phosphorane do not show cooperative catalysis.

(3) What is unique from the data shown in Table 3 is the considerably larger transition-state stabilization obtained from the cooperative interaction between the two Zn(II) centers in $[\text{Zn}_2(\text{L1})(\text{OH})_2]^{3+}$ relative to that observed for $[\text{Eu}_2(\text{L4})_2(\text{OH})(\text{H}_2\text{O})_2]^+$. The organization of metal cations by interaction with the bridging alkoxide ion reduces the entropic barrier for binding to the substrate compared to that for the interaction of loosely tethered complexes such as $[\text{Zn}_2(\text{L3})(\text{OH}_2)]^{4+}$. This is probably the key to the high activity for this complex because it facilitates interaction of both Zn(II) centers with the transition state. The absence of an analogous cooperative stabilization of the transition state for the cleavage of HpPNP by interactions with the Eu(III) centers in $[\text{Eu}_2(\text{L4})_2(\text{OH})(\text{H}_2\text{O})_2]^+$ may reflect the nonrigidity of a complex connected by a single hydroxide bridge as well as the relative inaccessibility of the Eu(III) cations for interaction with the charged substrate. In the dimeric catalyst, each Eu(III) center is bound to a septadentate ligand and a bridging hydroxide so that there is, at most, a single coordination site on each Eu(III) for interaction with the substrate. The unavailability of binding sites for substrate interaction severely attenuates the catalytic activity of related Eu(III) macrocyclic complexes.⁴⁷

A key component of most effective lanthanide(III) catalysts for RNA cleavage is their neutral ligand containing weak

Ln(III) donor groups including alcohols, amines, and amides.^{48–54} These weak donors are used in multidentate chelating macrocyclic ligands to produce complexes that are resistant to dissociation. Carboxylate containing ligands such as L4 are much stronger donors for Ln(III) and, consequently, may either attenuate catalysis as shown here or completely arrest it if used as part of a multidentate ligand. However, the judicious use of only a single carboxylate per Ln(III) ion in bidentate chelates produces dimeric catalysts that are quite active.¹⁹ The structures of these neutral dinuclear complexes are not fully characterized but include at least two bridging groups including hydroxide and, in some cases, an amino acid. Importantly, the bidentate ligands leave open multiple coordination sites for interaction with the substrate, and the presence of two bridging groups imparts a rigid framework for the dinuclear Ln(III) core. The strong interaction of these dinuclear amino acid complexes with anions is consistent with the ca. 10-fold higher activity of the Dy(III) or Nd(III) complex compared to that of the dinuclear Eu(III) complex studied here. The major drawback of such catalysts is that they are readily perturbed by the addition of other anions and ligands. On the basis of this analysis, constructing an efficient Ln dinuclear catalyst involves forming a rigid dinuclear framework with a highly accessible coordination sphere and a sufficient number of donor groups to prevent dissociation of the lanthanide ion. Such a balance is difficult to accomplish, but as is clear from these initial data, it will lead to more effective dinuclear catalysts than those currently available with dinuclear complexes of Zn(II).

Acknowledgment. J.R.M. and J.P.R. gratefully acknowledge the National Science Foundation (grant CHE0415356) for support of this work.

Supporting Information Available: pH–Potentiometric titration curves, equilibria and formation constants, and NMR spectra. This material is available free of charge via the Internet at <http://pubs.acs.org>.

IC7005666

- (42) Fanning, A.-M.; Plush, S. E.; Gunnlaugsson, T. *Chem. Commun.* **2006**, 3791–3793.
- (43) Gunnlaugsson, T.; Davies, R. J. H.; Nieuwenhuyzen, M.; Stevenson, C. S.; Viguier, R.; Mulready, S. *Chem. Commun.* **2002**, 2136–2137.
- (44) Gunnlaugsson, T.; O'Brien, J. E.; Mulready, S. *Tetrahedron Lett.* **2002**, 43, 8493–8497.
- (45) Amin, S.; Voss, D. A., Jr.; Horrocks, W. D., Jr.; Morrow, J. R. *Inorg. Chem.* **1996**, 35, 7466–7467.
- (46) Amin, S.; Morrow, J. R.; Lake, C. H.; Churchill, M. R. *Angew. Chem., Int. Ed. Engl.* **1994**, 33, 773–775.
- (47) Amin, S.; Voss, D. A., Jr.; Horrocks, W. D., Jr.; Lake, C. H.; Churchill, M. R.; Morrow, J. R. *Inorg. Chem.* **1995**, 34, 3294–3300.

- (48) Iverson, B. L.; Shreder, K.; Král, V.; Smith, D. A.; Smith, J.; Sessler, J. L. *Pure Appl. Chem.* **1994**, 66, 845–850.
- (49) Magda, D.; Crofts, S.; Lin, A.; Miles, D.; Wright, M.; Sessler, J. L. *J. Am. Chem. Soc.* **1997**, 119, 2293–2294.
- (50) Magda, D.; Miller, R. A.; Sessler, J. L.; Iverson, B. L. *J. Am. Chem. Soc.* **1994**, 116, 7439–7440.
- (51) Magda, D.; Wright, M.; Crofts, S.; Lin, A.; Sessler, J. L. *J. Am. Chem. Soc.* **1997**, 119, 6947–6948.
- (52) Canaple, L.; Hüsken, D.; Hall, J.; Häner, R. *Bioconjugate Chem.* **2002**, 13, 945–951.
- (53) Häner, R. *Chimia* **2001**, 55, 1035–1037.
- (54) Hüsken, D.; Goodall, G.; Blommers, M. J. J.; Jahnke, W.; Hall, J.; Häner, R.; Moser, H. E. *Biochemistry* **1996**, 35, 16591–16600.